EXHIBIT 86

Journal of Alzheimer's Disease 22 (2010) 235–245
DOI 10.3233/JAD-2010-100585
IOS Press

Alzheimer's Disease-Linked Presenilin Mutation (*PS1M146L*) Induces Filamin Expression and γ-Secretase Independent Redistribution

Qun Lu[a,b,*], Kai Ding[c], Matthew P. Frosch[d], Shiloh Jones[b], Michael Wolfe[c], Weiming Xia[c] and George W. Lanford[b]

[a]*Harriet and John Wooten Laboratory for Alzheimer's Disease and Neurodegenerative Diseases Research, The Brody School of Medicine, East Carolina University, Greenville, NC, USA*
[b]*Department of Anatomy and Cell Biology, The Brody School of Medicine, East Carolina University, Greenville, NC, USA*
[c]*Center for Neurologic Diseases, Brigham and Women's Hospital, Harvard Medical School, Boston, MA, USA*
[d]*C. S. Kubik Laboratory for Neuropathology, Massachusetts General Hospital, Harvard Medical School, Boston, MA, USA*

Handling Associate Editor: Thomas Shea

Accepted 11 June 2010

Abstract. Presenilin mutations are linked to the early onset familial Alzheimer's disease (FAD) and lead to a range of neuronal changes, indicating that presenilins interact with multiple cellular pathways to regulate neuronal functions. In this report, we demonstrate the effects of FAD-linked presenilin 1 mutation (*PS1M146L*) on the expression and distribution of filamin, an actin cross-linking protein that interacts with PS1 both physically and genetically. By using immunohistochemical methods, we evaluated hippocampal dentate gyrus for alterations of proteins involved in synaptic plasticity. Among many proteins expressed in the hippocampus, calretinin, glutamic acid decarboxylase (GAD67), parvalbumin, and filamin displayed distinct changes in their expression and/or distribution patterns. Striking anti-filamin immunoreactivity was associated with the polymorphic cells of hilar region only in transgenic mice expressing *PS1M146L*. In over 20% of the *PS1M146L* mice, the hippocampus of the left hemisphere displayed more pronounced upregulation of filamin than that of the right hemisphere. Anti-filamin labeled the hilar neurons only after the *PS1M146L* mice reached after four months of age. Double labeling immunohistochemical analyses showed that anti-filamin labeled neurons partially overlapped with cholecystokinin (CCK), somatostatin, GAD67, parvalbumin, and calretinin immunoreactive neurons. In cultured HEK293 cells, PS1 overexpression resulted in filamin redistribution from near cell peripheries to cytoplasm. Treatment of CHO cells stably expressing PS1 with WPE-III-31C or DAPT, selective γ-secretase inhibitors, did not suppress the effects of PS1 overexpression on filamin. These studies support a γ-secretase-independent role of PS1 in modulation of filamin-mediated actin cytoskeleton.

Keywords: Actin, dentate gyrus, filamin, hilar neurons, presenilin mutation, γ-secretase

*Correspondence to: Qun Lu, PhD., Department of Anatomy and Cell Biology, The Brody School of Medicine at East Carolina University, Greenville, NC 27834, USA. Tel.: +1 252 744 2844; Fax: +1 252 744 2850; E-mail: luq@ecu.edu.

INTRODUCTION

Presenilin (PS1 and PS2) mutations account for the majority of human familial Alzheimer's disease (FAD) cases. PS1 displays more than 150 mutations linked to aggressive forms of early onset FAD [1,2]. PS1 is often coupled with the γ-secretase activity that cleaves a number of substrates, including amyloid-β protein precursor (AβPP), Notch, CD44, and E-cadherin, to name just a few [3–7]. PS1 overexpression promoted the production of Aβ_{42} [8], and the PS1 knockout mice showed reduced Aβ_{42} production [9] and Aβ secretion [10]. On the other hand, PS1 is involved in the regulation of protein functions that could be dependent or independent of γ-secretase activity [11]. PS1 regulations also include protein-protein interactions that could be dependent or independent of FAD mutations [12–14]. Both γ-secretase dependent and independent activities of PS1 seem to act at the top of the signaling chains of events during development and aging, suggesting that PS1 controls many cellular pathways [15]. Among these cellular events, synaptic modulation of PS1 functions has caught much attention because a PS1-mediated synaptic alteration provides rationales for the neuronal defects associated with AD phenotypes [16–18].

Actin cytoskeleton is an important element in synaptic plasticity because it helps to stabilize the synaptic junction and is also responsible for the dynamic remodeling that occurs in response to stimuli [19,20]. It was demonstrated that PS1 interacts with cytoskeleton and associates with actin filaments [21]. Zhang et al. [12] first reported that PS1 interacts directly with filamin, an actin cross-linking protein. The evidence of interaction between filamin and PS1 is unequivocal, since a number of studies showed that PS1 interacts with filamin upon cellular adhesion to extracellular matrix [22] and the interaction occurs in *Drosophila* both physically and genetically [23]. The association between filamin and AD is also plausible, since filamin is detected in the neurofibrillary tangles and reactive microglia [12].

In this report, we provide further evidence supporting filamin as the potential target of PS1 signaling. We demonstrate a striking filamin expression in the polymorphic cells of the hilar region in transgenic mice expressing *PS1M146L*. The upregulation of filamin revealed unique features in that over 20% of the *PS1M146L* mice showed a more pronounced overexpression in the hippocampus of the left hemisphere than that of the right hemisphere, and its expression is developmentally regulated in *PS1M146L* mice. Double labeling immunohistochemical analyses showed that anti-filamin labeled neurons partially overlapped with CCK, somatostatin, GAD67, parvalbumin, and calretinin immunoreactive neurons. In cultured HEK293 cells, PS1 overexpression resulted in filamin redistribution from near cell surface to cytoplasm. Treatment of CHO cells overexpressing PS1 with WPE-III-31C or DAPT, selective γ-secretase inhibitors, did not suppress the effects of PS1 overexpression on filamin. These studies support a γ-secretase-independent role of PS1 in modulation of filamin and actin cytoskeleton.

MATERIALS AND METHODS

Antibodies and other materials

Antibodies used for the detection of δ-catenin were described previously [24]. The sources of other antibodies are as follows: rabbit anti-CCK, rabbit anti-somatostatin 28, rabbit anti-calretinin, rabbit anti-GFAP, and mouse anti-filamin (MAB1678, Millipore); anti-GAD67, anti-parvalbumin, anti-NF-κB, and anti-PSD95 (BD Bioscience); anti-NF-2, and anti-ChaT (Santa Cruz Biotechnology); Mouse anti-actin (EMD Bioscience); mouse anti-synaptophysin (p38), and anti-MAP2 (Sigma). Unless otherwise indicated, all other chemicals were from Sigma.

Cell culture and transfection

Primary hippocampal neuronal cultures were prepared as described by Banker and Goslin [25] with minor modifications [26]. Briefly, 18-day timed pregnant rats were sacrificed, and the embryos were removed in accordance with the NIH Guide for the Care and Use of Laboratory Animals. Hippocampi were collected, and cells were dissociated by trypsinization and plated onto poly-L-lysine coated glass coverslips. After neurons adhered to the substrate, the medium was changed to B-27 supplemented Neurobasal (Invitrogen, Carlsbad, CA). This culture scheme allowed us to maintain viable low-density cultures for several weeks. Neurons were grown for 1 day in vitro (DIV) and then treated with or without 300 nM WPE-III-31C (presenilin/γ-secretase inhibitor [27]), for 6 days. On 7 DIV, neurons were fixed in 4% paraformaldehyde for 15 minutes at 37°C.

Human embryonic kidney (HEK) 293 cells were cultured in Dulbeccos modified Eagles medium (DMEM) supplemented with 10% fetal bovine serum (FBS) and penicillin/streptomycin at 37°C with 5% CO_2.

The cells were transiently transfected with *PS1wt* and *PS1M146L* using Lipofectamine 2000 reagent as described by the manufacturer (Invitrogen). Chinese Hamster Ovary (CHO) cells stably expressing *PS1M146L* were grown in DMEM with 10% FBS and 12 μg/ml L-proline. Transgene expression was stably selected in the presence of Zeocin and G418 [28].

Immunofluorescence light microscopy

Neurons and HEK293 cells were fixed for immunofluorescent light microscopic experiments. Cells were treated with 0.2% Triton X-100 in PBS pH 7.4 for 15 min, blocked with 10% BSA for 30 min, and stained with FITC phalloidin (Molecular Probes, Inc, Eugene, OR) for neurons. HEK293 cells were double labeled using mouse monoclonal anti-filamin (Millipore) and rabbit anti-PS1 (Sigma, St Louis, MO). After PBS washes, nuclear morphology was assessed by staining with 0.2 μg/ml Hoechst 33258 (Sigma, St Louis, MO). The coverslips were mounted and analyzed with a Zeiss Axiovert S100 inverted fluorescent light microscope (Carl Zeiss, Thornwood, NY) equipped with MetaMorph imaging software.

Transgenic mice

Transgenic mice expressing *PS1* cDNAs (*wt* or $M146L$ mutation) under the control of a portion of the human platelet-derived growth factor (PDGF) B-chain promoter [29] were generated and maintained as described before [29]. To determine the genotypes of transgenic animals, PCR reactions were performed with three primers: a forward PCR primer (5'-GGCCAGAAGAGGAAAGGCT-3') that anneals equally well to the endogenous mouse and human PDGF B-chain promoter portion of the transgene and two reverse primers specific to either the *PS1* cDNA (5'-GTACAGTATTGCTCAGGTGGTTGT-3') or the mouse genomic PDGF B-chain gene (5'-AGTCTGCTATCTACCCACTCGCT-3'). The PCR reaction reveals 521 and 355 bp for transgene and endogenous mouse gene products, respectively. Two independent *PS1M146L* transgenic lines (*PS1M146La* with lower PS1 expression and *PS1M146Lb* with higher PS1 expression) were used in the current study to confirm that our observations were not derived from a particular *PS1M146L* transgenic line. Both the male and female mice were used in the study, and no significant differences in experimental outcomes were observed.

Immunohistochemistry

Transgenic mice were deeply anesthetized and perfused with 30 ml of ice-cold sodium nitrite. Immediately, the mouse was perfused with freshly prepared, chilled 4% paraformaldeyde. Whole brains were rapidly removed and placed in 4% paraformaldehyde/30% sucrose in PBS solution overnight at 4°C for fixation and cryoprotection. The tissue was embedded in OCT and rapidly frozen using liquid nitrogen chilled isopentane. 40 μm frozen brain coronal sections were affixed to Superfrost (Fisher Scientific, Pittsburgh, PA) slides and they were immunostained with appropriate primary antibodies described in the result section using the Vectastain ABC method (Vector Labs, Southfield, MI) with or without hematoxylin/eosin counterstaining. ABC staining was performed according to the manufacturer's suggestions. Double labeling immunohistochemistry was performed by sequential application of two primary antibodies followed by either peroxidase or alkaline phosphatase conjugated secondary antibodies. Some sections were stained by simple Nissl method.

Cell lysate preparation and immunoblotting

We prepared cell lysates from cell cultures and transgenic mouse brain hippocampi in RadioImmuno Precipitation Assay (RIPA) buffer (150 mM NaCl, 10 mM HEPES pH 7.3, 2 mM EDTA, 0.2% SDS, 0.5% Sodium deoxycholate, 1% Triton X-100) supplemented with protease inhibitors (Roche Complete Protease Inhibitor cocktail), followed by 30 min incubation on ice. Cell debris was removed by 14,000 g centrifugation. Supernatant was collected and protein concentration was determined using Pierce BCA assay. The samples were solubilized with 2X SDS sample buffer and loaded onto SDS-PAGE gels, transferred to nitrocellulose membrane, and subject to Western blot analysis with appropriate primary antibodies as described in the result section. Membranes were washed and then incubated in secondary antibody (1:2500 for all HRP) for 1 h at room temperature. After the membranes were washed, they were incubated with ECL Western detection reagents and then exposed to Blue Devil films (Genesee Scientific, San Diego, CA).

RESULTS

Immunohistochemical profiles of protein expression in hippocampal formation in PS1 transgenic mice

We examined the hippocampal morphology of transgenic mice (7 to 12 month old) expressing wild type

Table 1
Immunohistochemical profiling of proteins showing changes in expression and/or distribution specific for *PS1* or *PS1M146L* transgenic mice when compared to non-transgenic mice

Protein marker	PS1 Expression (Δ)	PS1 Distribution (Δ)	PS1M146L Expression (Δ)	PS1M146L Distribution (Δ)
Filamin	–	–	*	N/A
ChaT	–	–	–	–
Calretinin	+	+	+	N/A
GAD67	+	+	+	N/A
Parvalbumin	–	–	*	*
Synaptophysin	–	–	–	–
PSD95	+	+	+	N/A
δ−catenin	–	–	–	–
MAP2	–	–	–	–
NF-2	–	–	–	–
GFAP	–	–	–	–
NF-κB	–	–	–	–
Somatostatin	–	–	–	–
CCK8	–	–	–	–

Note: + Changes seen compared to non-transgenic mice.
* Changes seen between *PS1* or *PS1M146L* transgenic mice.
N/A-not applied.

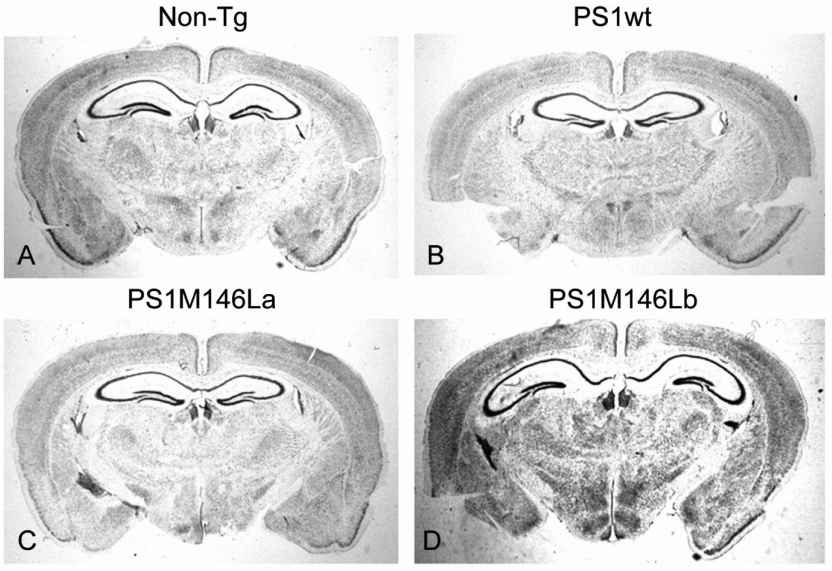

Fig. 1. Overall brain structures of 7–12 month old non-transgenic mice and PS1 transgenic mice. Nissl staining of the coronal brain sections showed that non-transgenic (A), transgenic mice expressing wild type PS1 (B) or transgenic mice expressing PS1M146L mutation (C, low expression transgenic line PS1M146L*a* and D, high expression transgenic line PS1M146L*b*) developed normal gross architecture of the hippocampus. X20.

human PS1 and PS1 expressing an AD mutation (*PS1M146L*). Nissl staining of the coronal brain sections showed that non-transgenic, as well as PS1 transgenic mice developed normal gross architecture of the hippocampus (Fig. 1). We then sought to apply immunohistochemistry to profile the expression of proteins that were known to influence neuronal functions in the hippocampus. We focused on the dentate gyrus and CA4 region, as neurons in this region are well known for their sensitivity to activity-dependent damages. Among all the protein markers we examined, we found no significant changes in the expression and distribution pattern for p38 synatophysin, choline acetyltransferase (ChaT), cholecystokinin (CCK8), NF-kappa, Glial fibrillary acidic protein (GFAP), neurofibromatosis Type 2 (NF-2), microtubule-associated protein 2 (MAP2), δ-catenin, somatostatin and parvalbumin (Table 1). While no distinct morphological changes were

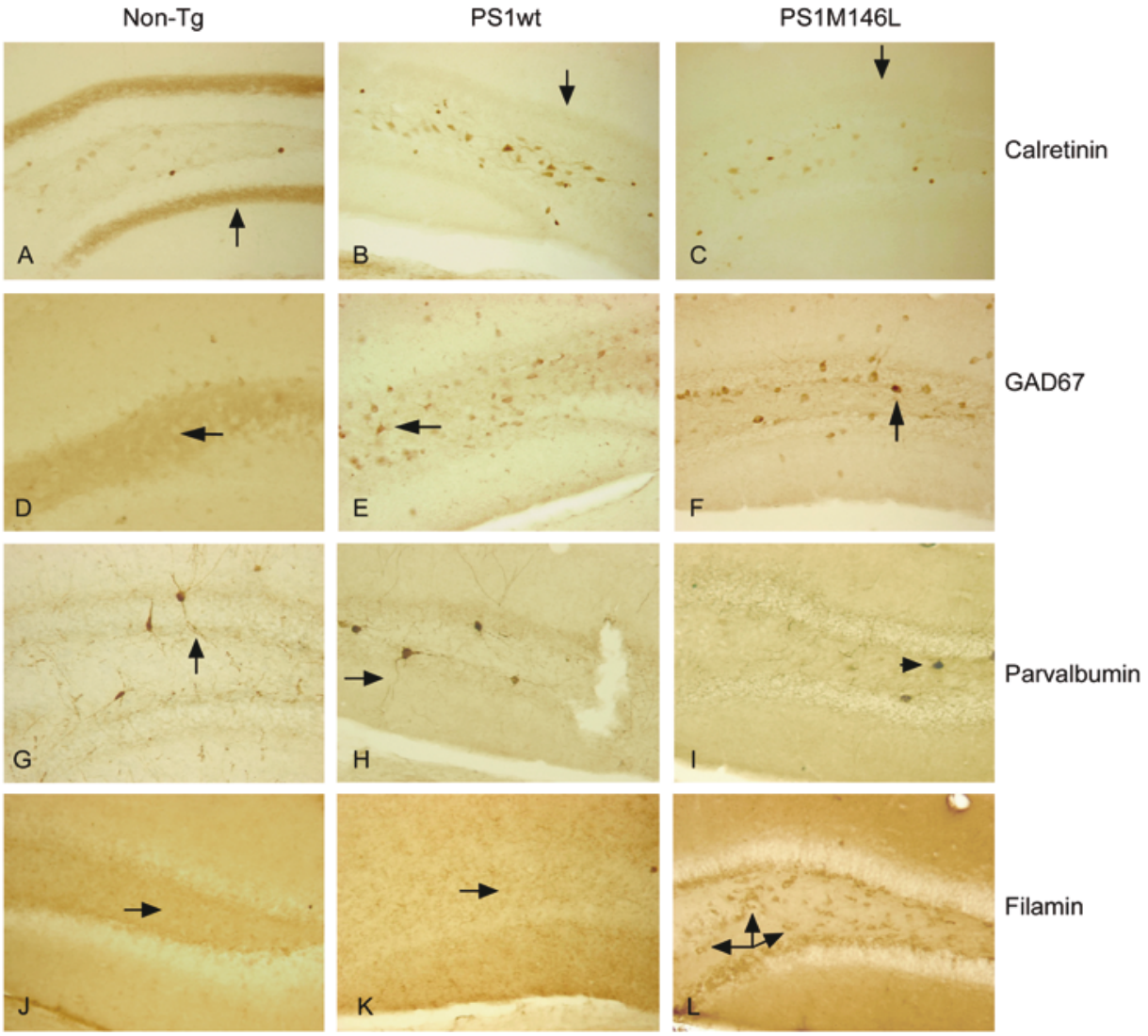

Fig. 2. Immunohistochemistry showing changes of expression in calretinin, GAD67, parvalbumin or filamin in dentate gyrus of hippocampus. A-C) Calretinitn. Arrows: the dentate gyrus supragranular layer (DGSL) is immunoreactive in non-transgenic (A), but not in PS1 wt (B) or PS1M146L transgenic mice (C); D-F. GAD67. Arrows: dentate hilar neurons are GAD67 immunoreactive in PS1 wt (E) and PS1M146L (F), but not in non-transgneic mice (D); G-I. Parvalbumin. Arrows: dentate hilar neurons immunoreactive to anti-parvalbumin show clear neuronal processes in non-transgenic (G) and PS1 wt (H), but not in PS1M146L transgenic mice (I, arrowhead); J-L. Filamin. Arrows: dentate hilar neurons are not immunoreactive to anti-filamin in non-transgenic (J) and PS1 wt transgenic mice (K), but immunoreactive to anti-filamin in PS1M146L transgenic mice (L). X50.

observed in the CA4 region, calretinin immunoreactivity was diminished in the dentate gyrus supragranular layers of *PS1* wild type and *PS1M146L* mouse brain (Fig. 2A-C: arrows). Glutamic acid decarboxylase (GAD67) immunoreactivity appeared to be increased in the *PS1* transgenic mice, but there were no differences between the wild type *PS1* and *PS1M146L* mice (Fig. 2D-F). While parvalbumin expression was observed in non-transgenic, *PS1* wild type and *PS1M146L* transgenic mice, its distribution was restricted to cell bodies in *PS1M146L* mice (Fig. 2I: arrowheads) when compared to control and PS1 wild type littermates where the immunoreactivity extended to the neurites (Fig. 2G-H: arrows). Most striking changes were observed in the expression of filamin, an actin cross-linking protein known to interact with PS1 physically, genetically, and functionally [12,23]. Control non-transgenic as well as wild type *PS1* expressing trans-

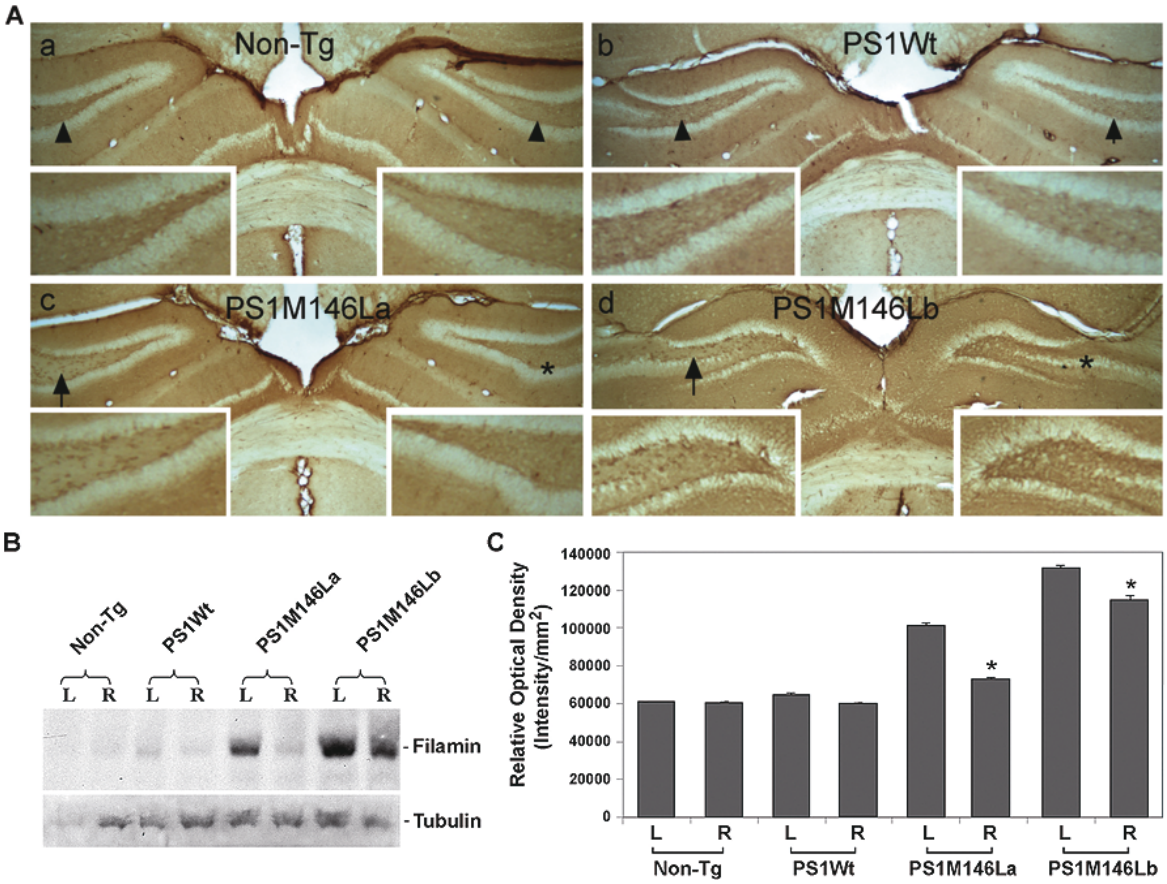

Fig. 3. Hemisphere-dependent distribution of filamin overexpression in PS1M146L transgenic mice. A) Immunohistochemical light microscopy showing that filamin expression was very weak in non-transgenic (a) and PS1 wt transgenic mice (b), but was very strong (arrow) in PS1M146L transgenic mice (c). Note: there were no differences in immunoreactivites in both the left and right hippocampi (arrowheads) in non-transgenic (a) and PS1 wt transgenic mice (b). However, hilar neurons were intensely labeled in the left (arrow), but not right hippocampus (asterisk) of PS1M146L transgenic mice (c and d). Inserts: higher magnification images of the respective hippocampi from a, b, c, and d. X50. B) Western blot showing that filamin immunoreactviies are more pronounced in the left (L) hippocampus than that in the right (R) hippocampus of PS1M146L transgenic mice. Individual hippocampus from non-transgenic, PS1 wt, or PSM146L transgenic mice were dissected and lysed. Proteins of equal loading were analyzed by Western blots. Anti-tubulin immunoreactivities were used as loading control. C) Semi-quantitative analysis of Western blot showing that filamin immunoreactivities are more pronounced in the left (L) hippocampus than in the right (R) hippocampus of PS1M146L transgenic mice (indicated by $*p < 0.05$). This experiment was repeated with two sets of low expression (*PS1M146La*) and high expression (*PS1M146Lb*) mice.

genic mice did not display neuronal staining in the dentate gyrus and CA4 area (Fig J-K). However, large, polymorphic hilar neurons showed strong immunoreactivity for filamin in *PS1M146L* mouse brains (Fig 2L: arrows).

Bilateral hemisphere asymmetry and developmental regulation of filamin expression in PS1M146L transgenic mice

We further investigated the filamin expression and distribution in the hilar region (Fig. 3A). Consistent with the data shown in Fig. 2J and K, filamin expression was not detected in non-transgenic mice (Fig. 3A, a: arrowheads; also see the insert) and transgenic mice expressing wild type PS1 (Fig. 3A, b: arrowheads; also see the insert). However, when filamin distribution in mouse brains of two independent *PS1M146L* transgenic lines was examined, we found that the hippocampus on the left side of the brain showed stronger immunostaining (Fig. 3A, c and d: arrows; also see the insert) than on the right side (Fig. 3A, c and d: asterisks; also see the inserts). We have examined a total of 25 *PS1M146L* mice by immunohistochemical method and observed left and right asymmetry in filamin expression in the dentate gyrus in over 20% of the mice. The same

observation of hilar filamin expression was observed in two *PS1M146L* transgenic mouse lines (*PS1M146La* with lower PS1 expression and *PS1M146Lb* with high PS1 expression, see Fig. 3A, c and d).

To confirm the results of immunohistochemical study, we dissected and separated the hippocampi from the two hemispheres. Protein lysates were prepared and Western blots were performed. No filamin immunoreactivities were detected in the control, non-transgenic mouse hippocampi (Fig. 3B). Hippocampus of the *PS1* wild type transgenic mouse showed weak detection for filamin immunoreactivity. However, we detected strong filamin immunoreactivity in two independent lines of transgenic mice expressing *PS1M146L* (Fig. 3B). Furthermore, Western blot as well as semi-quantification analyses (Fig. 3C) showed that the left hippocampus displayed consistently more intense immunoreactivity than that of right hippocampus confirming the observation from immunohistochemical analyses.

We further examined the onset of filamin expression in hilar neurons during mouse development. Interestingly, no filamin immunoreactivity was detected in *PS1M146L* transgenic mice until they reach 4 month of age, suggesting that the *PS1M146L*-induced filamin expression is either developmentally regulated or requires cooperation of co-factors.

Partial co-distribution of filamin with CCK, Somatostatin, GAD67, Parvalbumin, and Calretinin immunoreactive neurons in the hilar region of PS1M146L transgenic mice

To explore the potential identity of the hilar neurons that were immunoreactive with anti-filamin in *PS1M146L* transgenic mice, we double labeled *PS1M146L* brain slices with anti-filamin and antibodies recognizing subsets of hilar neurons. Anti-CCK was known to label hilar basket neurons [30] and stained these types of neurons in *PS1M146L* mouse brain (Fig. 4A, arrows). Double labeling analysis showed that the CCK immunoreactive neurons were also reactive with anti-filamin (Fig. 4B, arrowheads), although filamin was expressed in a wider range of hilar neurons than CCK expressing neurons. Somatostatin was expressed in many hilar neurons (Fig. 4C, arrows) and showed good co-distribution with filamin (Fig. 4D, arrowheads). But some neurons immunoreactive with anti-filamin did not show somatostatin immunoreactivity (Fig. 4D, asterisk). Compared to filamin immunoreactive neurons (Fig. 4E, arrows), anti-GAD67

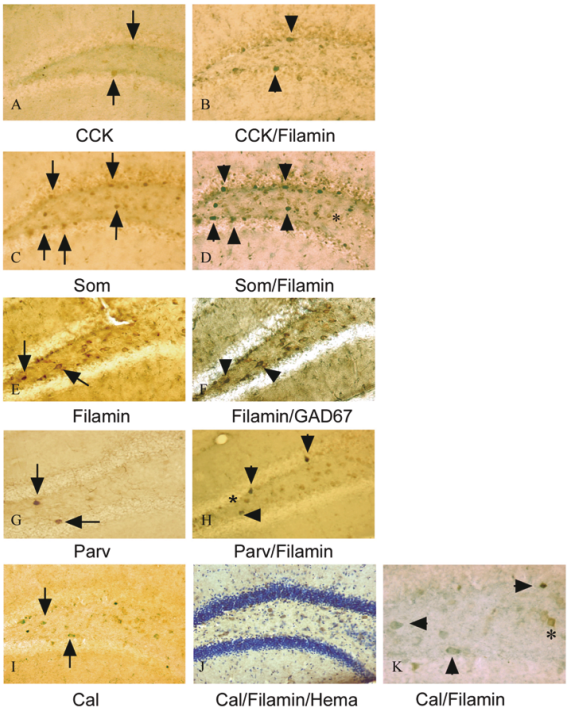

Fig. 4. Partial co-distribution of filamin with other proteins of dentate gyrus in PS1M146L mouse brain. A) CCK. B) Double labeling with anti-CCK followed by anti-filamin. Arrows and arrowheads: examples of neurons showing CCK and filamin co-distribution. C) Somatostatin. D) Double labeling with anti-somatostatin (Som) followed by anti-filamin. Arrows and arrowheads: examples of neurons showing somatostatin and filamin co-distribution. Asterisk indicates non-overlapping staining in some neurons. E) Filamin. F) Double labeling with anti-filamin followed by anti-GAD67. Arrows and arrowheads: examples of neurons showing filamin and GAD67 co-distribution. G) Parvalbumin. H) Double labeling with anti-parvalbumin (Parv) followed by anti-filamin. Arrows and arrowheads: examples of neurons showing partial parvalbumin and filamin co-distribution. Asterisk indicates non-overlapping staining in some neurons. I) Calretinin. J) Triple labeling of anti-calretinin (Cal), anti-filamin, and hematoxylin. K) Double labeling with anti-calretinin (Cal) followed by anti-filamin. Arrows and arrowheads: examples of neurons showing partial calretinin and filamin co-distribution. Asterisk indicates a neuron immunoreactive only to anti-calretinin. X50.

recognized some but not all neurons expressing filamin (Fig. 4F, arrowheads). Here, staining with anti-filamin first during the double labeling immunohistochemical procedure allowed clear visualization of cytoplasmic filamin distribution in the hilar neurons (Fig. 4E, arrows).

Very few neurons expressed parvalbumin in the hilar region (Fig. 4G, arrows). However, double labeling showed that some neurons immunoreactive with anti-parvalbumin also reacted with anti-filamin (Fig. 4H, arrowheads). Anti-calretinin recognized many hilar neurons (Fig. 4I, arrows; Fig. 2A-C) some of which

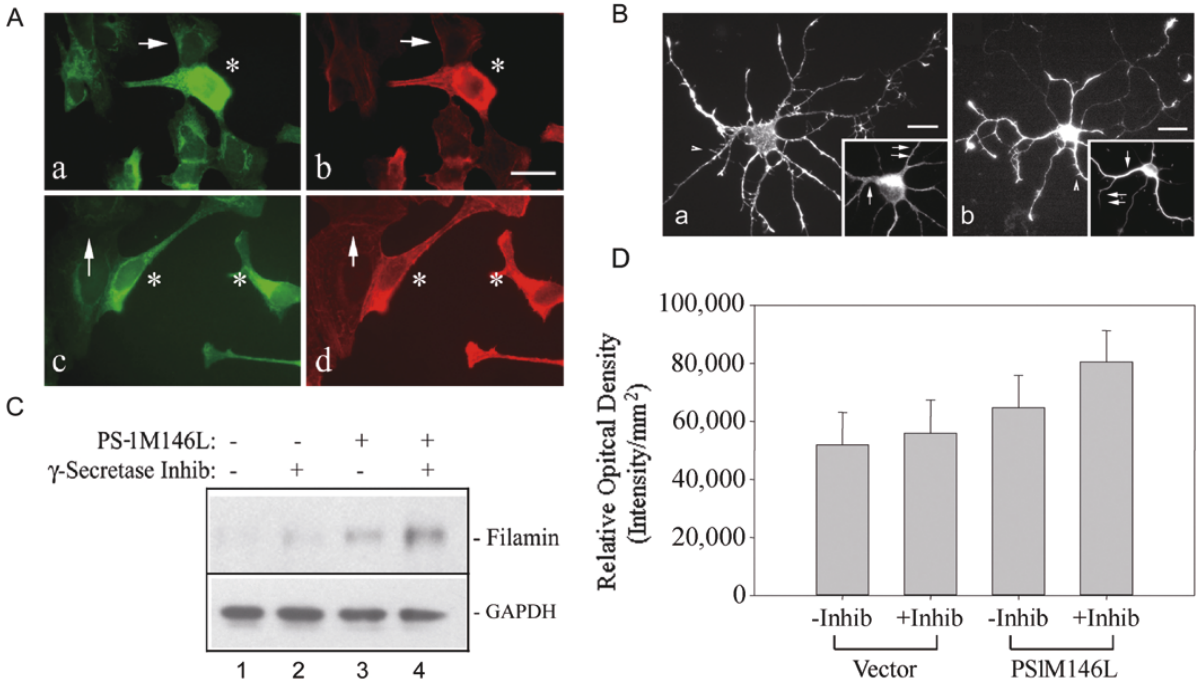

Fig. 5. γ-Secretase-independent, PS1M146L-induced filamin expression and re-distribution. A) Double labeling using laser confocal immunofluorescent light microscopy of HEK293 cells transiently overexpressing PS1M146L. a and b) HEK293 cells transfected with PS1M146L without treatment of γ-secretase inhibitor WPE-III-31C. a) Anti-PS1 staining of cells overexpressing PS1 (asterisk) and cells expressing basal level of PS1 (arrow). b) Anti-filamin staining of the same cells as in *a* with the cells overexpressing PS1 (asterisk) and cells expressing basal level of PS1 (arrow). Note: anti-filamin immunoreactivities were restricted to the cell periphery in cells expressing basal PS1 (arrow in b) but re-distributed to the cytoplasm in the cells overexpressing PS1 (asterisks in b). c and d) HEK293 cells transfected with PS1M146L with treatment of 300 nM γ-secretase inhibitor WPE-III-31C. c. Anti-PS1 staining of cells overexpressing PS1 (asterisk) and cells expressing basal level of PS1 (arrow). d) Anti-filamin staining of the same cells as in *c* with the cells overexpressing PS1 (asterisk) and cells expressing basal level of PS1 (arrow). Note: weakened anti-filamin immunoreactivities to the cell periphery in cells expressing basal PS1 (arrow in d) whereas the filamin immunoreactivity remained in the cytoplasm of cells overexpressing PS1 (asterisks in d). Bar: 20 μm. B) Increased extension of neurites in hippocampal neurons treated with γ-secretase inhibitor WPE-III-31C. a) Phalloidin fluorescent staining showing F-actin-based neuronal morphology of control cells without treatment of WPE-III-31C. Arrows point to neuronal branches (Insert: MAP2 immunostaining of dendrites with double arrows pointing to branching). Bar: 10 μm. b) Phalloidin fluorescent staining showing F-actin-based neuronal morphology of cells with treatment of WPE-III-31C. Arrows point to neuronal branches (Insert: MAP2 immunostaining of dendrites). Bar: 15 μm. Note: neurites extended beyond the field in *b* even though photographed area was 50% larger than that in *a*. C) Western blots showing γ-secretase-independent filamin overexpression in CHO cells stably transfected with PS1M146L. CHO cells with or without PS1M146L transfection were lysed and proteins analyzed by anti-filamin. Anti-GAPDH immunoreactivity was used as loading control.

also reacted with anti-filamin (Fig. 4K, arrowheads), but others did not (Fig. 4K, asterisk). Compared to the total hilar neuronal populations indicated by H& E staining (Fig. 4J), anti-filamin labeled the mostly large, polymorphic neurons that co-distributed partially with CCK, somatostatin, GAD, parvalbumin, and calretinin immunoreactive cells (Fig. 4).

γ-Secretase-independent, PS1M146L-induced filamin expression and re-distribution

We next asked if *PS1M146L* could directly influence filamin expression and distribution at the cellular level. In human HEK293 cells showing a basal level of PS1 expression characteristic of endoplasmic reticulum (Fig. 5A, a: arrow), filamin distribution was largely restricted to the cell periphery where the subcortical actin cytoskeleton is usually enriched (Fig. 5A, b: arrow). However, in HEK 293 cells transiently transfected with *PS1M146L* (Fig. 5A, a: asterisk), filamin expression was enhanced and its distribution became peri-nuclear and cytoplasmic similar to that of PS1 (Fig. 5A, b: asterisk). The effects of *PS1wt* and *PS1M146L* on filamin redistribution in cultured cells were similar. However, since *PS1M146L* was known to display elevated γ-secretase activity and increase the production of $A\beta_{42}$, we applied γ-secretase in-

hibitor WPE-III-31C [27] to the cell cultures expressing *PS1M146L*. Treatment of HEK293 cells expressing *PS1M146L* (Fig. 5A, c: asterisks) with 300 nM WPE-III-31C did not alter the pattern of PS1M146L-induced filamin overexpression and redistribution (Fig. 5A, d: asterisks). The same regimen of WPE-III-31C treatment promoted neurite extension (Fig. 5B, b: arrowheads; also see arrows in the insert) when compared to untreated neurons (Fig. 5B, a arrowheads; also see arrows in the insert) as reported [31], verifying the efficacy of the inhibitor. It appeared that even the cells without PS1M146L expression also showed less pronounced distribution of filamin at the cell periphery (Fig. 5A, c and d: arrows), strongly suggesting that PS1M146L-induced filamin expression and redistribution is γ-secretase-independent. The same results of filamin expression and redistribution were obtained from CHO cells stably expressing PS1M146L treated with WPE-III-C31 or DAPT [32], another γ-secretase inhibitor (data not shown). In CHO cells stably expressing PS1M146L, Western blot and semi-quantification analyses showed increased filamin immunoreactivity when compared to vector transfected CHO cells (Fig. 5C, compare lane 1 with lane 3, and lane 2 with lane 4; Fig 5D). WPE-III-31C treatments did not attenuate or inhibit PS1M146L induced filamin expression (Fig. 5C, compare lane 1 with lane 2, and lane 3 with lane 4; Fig 5D). DAPT treatment showed similar results (data not shown). These studies again demonstrated that the increased filamin expression and its redistribution upon PS1M146L transfection were γ-secretase-independent.

DISCUSSION

PS1 is a pleiotropic protein that plays important roles in many cellular pathways. It is widely documented in the literature that PS1 interacts with filamin and the actin cytoskeleton [12,21–23]. Our observations are consistent with these studies.

It is interesting that changes in filamin expression in the CA4 region are developmentally regulated in PS1M146L mouse brain. It is not clear why the left hemisphere is more affected. One possibility is that the co-factors regulating filamin expression is specifically localized in the left hemisphere. Although PS1 transfection shows direct effects on filamin expression in HEK293 and CHO cells, the same effects are not shown in all neurons in the PS1M146L brain, indicating that filamin in hilar neurons is under cell-type specific regulation. Furthermore, filamin expression is not observed in PS1M146L embryogenesis, indicating that a transcription co-factor may be required that is developmentally regulated *in vivo* but is active constitutively in HEK293 and CHO cells in culture.

The significance of hilar expression of filamin and its co-expression with other hilar proteins, such as calretinin, CCK, somatostatin, parvalbumin, and GAD67 is not clear. Hilar neurons play important roles in hippocampal neural circuitry and are pivotally involved in seizures [33,34]. Accumulating evidence also suggests that these proteins may play roles in AD pathogenesis. For example, dystrophic calretinin immunoreactive fibers were often observed in the outer molecular layer of the dentate gyrus and in the CA4 sector in AD. There were also significantly increased numbers of small but decreased numbers of large parvalbumin and calretinin immunoreactive neuronal profiles in AD brain than in controls [35]. Most neurons containing neurofibrillary tangles were not calretinin immunoreactive, and most senile plaques were not associated with calretinin positive fibers, indicating that entorhinal calretinin-positive neurons may be affected in AD [36]. CCK is a peptide that can be found in the cerebral cortex in high concentrations and is involved in learning and memory as well as neurodegenerative processes. CCK, as well as somatostatin expression, is significantly reduced in AD [37]. γ-Aminobutyric acid (GABA), the principal inhibitory neurotransmitter of CNS, has been consistently implicated in the pathophysiology of many neurological disorders. GABA is synthesized from glutamate by the enzyme glutamic acid decarboxylase (GAD). Changes in GABAergic neurotransmission as represented by the GAD67 mRNA expression have been reported in extrapyramidal signs often observed in AD [38], although direct indication of GAD67 in the dentate gyrus has not been examined fully.

It is not clear what the potential consequences of filamin upregulation are in neurons or at the synapses. Filamin is a large actin cross-linking protein that is critical for the formation of lamellipodia at the leading edge of a migrating neuron. During cortical development, differentiating neurons rely on the filamin to initiate neuronal migration. Defective filamin due to gene mutation leads to failures in neuronal migration and sub-ventricular neuronal accumulation in periventricular heterotopia [39]. Because neuronal sprouting involves actin cytoskeleton in synaptic remodeling, it is possible that filamin plays important roles by modulating actin dynamics in synaptic plasticity. On the other

hand, recent studies showed that one of filamin's targets is the cell-cell junction [40]. Therefore, filamin may help bring together PS1 with other known PS1 binding proteins to the synaptic junction (e.g., E/N-cadherin and catenins). Because synaptic remodeling involves neuronal sprouting as well as actin cytoskeleton at the synapse, it is possible that filamin plays important roles by modulating actin dynamics and synaptic junction proteins. In our future studies, we will overexpress PS1 in neurons with or without filamin to determine whether filamin is required in PS1-mediated synaptic remodeling.

ACKNOWLEDGMENTS

We thank Melissa Clark and Christi Boykin for technical assistance. This study was supported in part by NIH/NIA (026630) and NIH/NCI (CA111891) grants (Q.L.).

Authors' disclosures available online (http://www.j-alz.com/disclosures/view.php?id=493).

REFERENCES

[1] Kim TW, Tanzi RE (1997) Presenilins and Alzheimer's disease. *Curr Opin Neurobiol* **7**, 683-688.

[2] De Strooper B (2007) Loss-of-function presenilin mutations in Alzheimer disease. Talking Point on the role of presenilin mutations in Alzheimer disease. *EMBO Rep* **8**, 141-146.

[3] De Strooper B, Saftig P, Craessaerts K, Vanderstichele H, Guhde G, Annaert W, Von Figura K, Van Leuven F (1998) Deficiency of presenilin-1 inhibits the normal cleavage of amyloid precursor protein. *Nature* **391,** 387-390.

[4] De Strooper B, Annaert W, Cupers P, Saftig P, Craessaerts K, Mumm JS, Schroeter EH, Schrijvers V, Wolfe MS, Ray WJ, Goate A, Kopan R (1999) A presenilin-1-dependent gamma-secretase-like protease mediates release of Notch intracellular domain. *Nature* **398**, 518-522.

[5] Okochi M, Steiner H, Fukumori A, Tanii H, Tomita T, Tanaka T, Iwatsubo T, Kudo T, Takeda M, Haass C (2002) Presenilins mediate a dual intramembranous gamma-secretase cleavage of Notch-1. *EMBO J* **21**, 5408-5416.

[6] Lammich S, Okochi M, Takeda M, Kaether C, Capell A, Zimmer AK, Edbauer D, Walter J, Steiner H, Haass C (2002) Presenilin-dependent intramembrane proteolysis of CD44 leads to the liberation of its intracellular domain and the secretion of an Abeta-like peptide. *J Biol Chem* **277**, 44754-44759.

[7] Marambaud P, Shioi J, Serban G, Georgakopoulos A, Sarner S, Nagy V, Baki L, Wen P, Efthimiopoulos S, Shao Z, Wisniewski T, Robakis NK (2002) A presenilin-1/gamma-secretase cleavage releases the E-cadherin intracellular domain and regulates disassembly of adherens junctions. *EMBO J* **21**, 1948-1956.

[8] . Duff K, Eckman C, Zehr C, Yu X, Prada CM, Perez-tur J, Hutton M, Buee L, Harigaya Y, Yager D, Morgan D, Gordon MN, Holcomb L, Refolo L, Zenk B, Hardy J, Younkin S (1996) Increased amyloid-beta42(43) in brains of mice expressing mutant presenilin 1. *Nature* **383**, 710-713.

[9] . Qian S, Jiang P, Guan XM, Singh G, Trumbauer ME, Yu H, Chen HY, Van de Ploeg LH, Zheng H (1998) Mutant human presenilin 1 protects presenilin 1 null mouse against embryonic lethality and elevates Abeta1-42/43 expression. *Neuron* **20**, 611-617.

[10] Naruse S, Thinakaran G, Luo JJ, Kusiak JW, Tomita T, Iwatsubo T, Qian X, Ginty DD, Price DL, Borchelt DR, Wong PC, Sisodia SS (1998) Effects of PS1 deficiency on membrane protein trafficking in neurons. *Neuron* **21**, 1213-1221.

[11] Parks AL, Curtis D (2007) Presenilin diversifies its portfolio. *Trends Genet* **23**, 140-150.

[12] Zhang W, Han SW, McKeel DW, Goate A, Wu JY (1998) Interaction of presenilins with the filamin family of actin-binding proteins. *J Neurosci* **18**, 914-922.

[13] Kang DE, Soriano S, Frosch MP, Collins T, Naruse S, Sisodia SS, Leibowitz G, Levine F, Koo EH (1999) Presenilin 1 facilitates the constitutive turnover of beta-catenin: differential activity of Alzheimer's disease-linked PS1 mutants in the beta-catenin-signaling pathway. *J Neurosci* **19**, 4229-4237.

[14] Kim JS, Bareiss S, Kim KK, Tatum R, Han JR, Jin YH, Kim H, Lu Q, Kim K (2006) Presenilin-1 inhibits delta-catenin-induced cellular branching and promotes delta-catenin processing and turnover. *Biochem Biophys Res Commun* **351**, 903-908.

[15] Wines-Samuelson M, Shen J (2005) Presenilins in the developing, adult, and aging cerebral cortex. *Neuroscientist* **11,** 441-451.

[16] Aoki C, Lee J, Nedelescu H, Ahmed T, Ho A, Shen J (2009) Increased levels of NMDA receptor NR2A subunits at pre- and postsynaptic sites of the hippocampal CA1: an early response to conditional double knockout of presenilin 1 and 2. *J Comp Neurol* **517,** 512-523.

[17] Selkoe DJ (2002) Alzheimer's disease is a synaptic failure. *Science* **298,** 789-791.

[18] Wang Y, Greig NH, Yu QS, Mattson MP (2009) Presenilin-1 mutation impairs cholinergic modulation of synaptic plasticity and suppresses NMDA currents in hippocampus slices. *Neurobiol Aging* **30,** 1061-1068.

[19] Rao A, Craig AM (2000) Signaling between the actin cytoskeleton and the postsynaptic density of dendritic spines. *Hippocampus* **10**, 527-541.

[20] Tada T, Sheng M (2006) Molecular mechanisms of dendritic spine morphogenesis. *Curr Opin Neurobiol* **16**, 95-101.

[21] Sych M, Hartmann H, Steiner B, Mueller WE (2000) Presenilin I interaction with cytoskeleton and association with actin filaments. *Neuroreport* **11**, 3091-3098.

[22] Schwarzman AL, Singh N, Tsiper M, Gregori L, Dranovsky A, Vitek MP, Glabe CG, St George-Hyslop PH, Goldgaber D (1999) Endogenous presenilin 1 redistributes to the surface of lamellipodia upon adhesion of Jurkat cells to a collagen matrix. *Proc Natl Acad Sci U S A* **96**, 7932-7937.

[23] Guo Y, Zhang SX, Sokol N, Cooley L, Boulianne GL (2000) Physical and genetic interaction of filamin with presenilin in Drosophila. *J Cell Sci* **113**, 3499-3508.

[24] Lu Q, Paredes M, Medina M, Zhou J, Cavallo R, Peifer M, Orecchio L, Kosik KS (1999) delta-catenin, an adhesive junction-associated protein which promotes cell scattering. *J Cell Biol* **144**, 519-532.

[25] Banker G, Goslin K (1988) Developments in neuronal cell culture. *Nature* **336,** 185-186.

[26] Jones SB, Lu HY, Lu Q (2004) Abl tyrosine kinase promotes dendrogenesis by inducing actin cytoskeletal rearrangements in cooperation with Rho family small GTPases in hippocampal neurons. *J Neurosci* **24,** 8510-8521.

[27] Esler WP, Das C, Campbell WA, Kimberly WT, Kornilova AY, Diehl TS, Ye W, Ostaszewski BL, Xia W, Selkoe DJ, Wolfe MS (2002) Amyloid-lowering isocoumarins are not direct inhibitors of gamma-secretase. *Nat Cell Biol* **4**, E110-1.

[28] Xia W, Zhang J, Kholodenko D, Citron M, Podlisny MB, Teplow DB, Haass C, Seubert P, Koo EH, Selkoe DJ (1997) Enhanced production and oligomerization of the 42-residue amyloid beta-protein by Chinese hamster ovary cells stably expressing mutant presenilins. *J Biol Chem* **272**, 7977-7982.

[29] Sasahara M, Fries JW, Raines EW, Gown AM, Westrum LE, Frosch MP, Bonthron DT, Ross R, Collins T (1991) PDGF B-chain in neurons of the central nervous system, posterior pituitary, and in a transgenic model. *Cell* **64**, 217-227.

[30] Acsády L, Katona I, Martínez-Guijarro FJ, Buzsáki G, Freund TF (2000) Unusual target selectivity of perisomatic inhibitory cells in the hilar region of the rat hippocampus. *J Neurosci* **20**, 6907-6919.

[31] Figueroa DJ, Morris JA, Ma L, Kandpal G, Chen E, Li YM, Austin CP (2002) Presenilin-dependent gamma-secretase activity modulates neurite outgrowth. *Neurobiol Dis* **9**, 49-60.

[32] Dovey HF, John V, Anderson JP, Chen LZ, de Saint Andrieu P, Fang LY, Freedman SB, Folmer B, Goldbach E, Holsztynska EJ, Hu KL, Johnson-Wood KL, Kennedy SL, Kholodenko D, Knops JE, Latimer LH, Lee M, Liao Z, Lieberburg IM, Motter RN, Mutter LC, Nietz J, Quinn KP, Sacchi KL, Seubert PA, Shopp GM, Thorsett ED, Tung JS, Wu J, Yang S, Yin CT, Schenk DB, May PC, Altstiel LD, Bender MH, Boggs LN, Britton TC, Clemens JC, Czilli DL, Dieckman-McGinty DK, Droste JJ, Fuson KS, Gitter BD, Hyslop PA, Johnstone EM, Li WY, Little SP, Mabry TE, Miller FD, Audia JE (2001) Functional gamma-secretase inhibitors reduce beta-amyloid peptide levels in brain. *J Neurochem* **76**, 173-181.

[33] Binaschi A, Bregola G, Simonato M (2003) On the role of somatostatin in seizure control: clues from the hippocampus. *Rev Neurosci* **14,** 285-301.

[34] Scharfman HE (2007) The CA3 "backprojection" to the dentate gyrus. *Prog Brain Res* **163**, 627-637.

[35] Leuba G, Kraftsik R, Saini K (1998) Quantitative distribution of parvalbumin, calretinin, and calbindin D-28k immunoreactive neurons in the visual cortex of normal and Alzheimer cases. *Exp Neurol* **152**, 278-291.

[36] Brion JP, Résibois A (1994) A subset of calretinin-positive neurons are abnormal in Alzheimer's disease. *Acta Neuropathol* **88**, 33-43.

[37] Mazurek MF, Beal MF (1991) Cholecystokinin and somatostatin in Alzheimer's disease postmortem cerebral cortex. *Neurology* **41**, 716-719.

[38] Boissière F, Faucheux B, Duyckaerts C, Hauw JJ, Agid Y, Hirsch EC (1998) Striatal expression of glutamic acid decarboxylase gene in Alzheimer's disease. *J Neurochem* **71**, 767-774.

[39] Fox JW, Lamperti ED, Ekşioğlu YZ, Hong SE, Feng Y, Graham DA, Scheffer IE, Dobyns WB, Hirsch BA, Radtke RA, Berkovic SF, Huttenlocher PR, Walsh CA (1998) Mutations in filamin 1 prevent migration of cerebral cortical neurons in human periventricular heterotopia. *Neuron* **21**, 1315-1325.

[40] Feng Y, Chen MH, Moskowitz IP, Mendonza AM, Vidali L, Nakamura F, Kwiatkowski DJ, Walsh CA (2006) Filamin A (FLNA) is required for cell-cell contact in vascular development and cardiac morphogenesis. *Proc Natl Acad Sci U S A* **103**, 19836-19841.